Engineering Analysis with Boundary Elements 128 (2021) 195–202

Contents lists available at ScienceDirect

Engineering Analysis with Boundary Elements

journal homepage: www.elsevier.com/locate/enganabound

Thermal analysis of electronic packaging structure using isogeometric boundary element method

Huiping Yu[a], Yubo Guo[a], Yanpeng Gong[a,b,*], Fei Qin[a,b]

[a] Institute of Electronics Packaging Technology and Reliability, Faculty of Materials and Manufacturing, Beijing University of Technology, Beijing 100124, China
[b] Beijing Key Laboratory of Advanced Manufacturing Technology, Faculty of Materials and Manufacturing, Beijing University of Technology, Beijing 100124, China

ARTICLE INFO

Keywords:
IGABEM
Electronic packaging structure
Radial integration method
Multi-scale property of geometry
Nearly singular integrals

ABSTRACT

The purpose of this paper is to carry out heat transfer analysis of integrated circuit (IC) packaging structures by the isogemoetric boundary element method (IGABEM). In service time, chips of electronic packaging structure produce lots of heat, which leads to resultant equations including domain integrals. In this work, the radial integration method is used to deal with domain integrals caused by the heat source. Since material properties of electronic packaging structure are piecewise continuous, the subregion isogemoetric boundary element method is introduced in the present IGABEM. In addition, the multi-scale property of structure leads to challenge of IGABEM analysis in electronic packaging problems. This largely results from the difficulty of integrating nearly singular integrals in an accurate and efficient manner. To deal with this problem, a hybrid nearly singular integration scheme, which delivers results of engineering accuracy in an optimal time is used in this work. Finally, a set of numerical examples demonstrate the ability of the present IGABEM to produce accurate temperature distributions.

1. Introduction

With integrated circuits (ICs) entering the age of More Moore, characteristics of electronic device are toward the trend of multi-material, multi-interface and high-density. Heat transfer problems with internal heat source have important applications in these problems, thus it is of great significance to find a precise and effective modeling method to solve these problems. Actually, many methods have been used to study heat transfer problems, such as analytical method [1], finite element method [2,3] and finite difference method [4]. Although great progresses have been achieved for each of above methods, these methods exist some drawbacks, e.g. (i) some methods are only suitable for special problems; (ii) some methods need a very refined mesh near the heat source or area with complex geometries. Since advantages of reduction dimensionality of the problem by one, only boundary discretization required and high accurate stress analysis, boundary element method (BEM) seems to be a promising method in heat transfer problems for electronic devices [5].

In 2002, Mera et al. [6] studied the anisotropic heat transfer problems by boundary element method and focused on the singularities in the method. Khatir and Lefebvre [7] investigated the thermal behavior of high power semiconductor packages subjected to power cycling loads by using boundary element method. And found that the accuracy of BEM has been satisfactorily evaluated by means of comparisons with experimental measurements in steady-state and transient operations. Shiah et al. [8] investigated the heat conduction in anisotropic composites with thin adhesive media by the boundary element method. Škerget et al. [9] studied the heat transport in multilayered composite pipe by boundary element method. In [10] the boundary element method was successfully used to study the thermomechanical contact problem in 3D microelectronic packaging. Based on boundary element method, Majchrzak and Turchan [11] studied laser heating problems for bi-layered microdomain. Recently, Gu and Zhang [12] presented a special crack-tip element to study interface crack by boundary element method.

In 2005, Hughes et al. [13] established a promising method called isogeometric analysis as a way of bridging the gap between Computer Aided Design (CAD) and Computer Aided Engineering (CAE). It was found that there are lots of benefits existing in this technology. Then this method has attracted a large research community and the isogeometric concept was used to many problems including functionally graded porous plates [14], shape optimization [15], anisotropic brittle fracture [16], heat transfer [17], etc.

Although it is possible to obtain geometrical data directly from the CAD program for Isogeometric Analysis (IGA), the implementation of IGA in solid models is not easy due to the requirement of volumetric Non-Uniform Rational B-Spline (NURBS). Then researches found that both the BEM and CAD define domains by bounding surfaces, which makes the integration of BEM and CAD much more natural. In 2012,

* Corresponding author at: Institute of Electronics Packaging Technology and Reliability, Faculty of Materials and Manufacturing, Beijing University of Technology, Beijing 100124, China.
E-mail address: yanpeng.gong@bjut.edu.cn (Y. Gong).

https://doi.org/10.1016/j.enganabound.2021.04.008
Received 3 January 2021; Received in revised form 1 March 2021; Accepted 12 April 2021

Simpson et al. [18] successfully applied the isogeometric concept in a BEM framework for elastic problems and formed the isogeometric boundary element method (IGABEM). Since IGABEM integrated the advantages of conventional BEM and IGA, this method was widely used for many applications, such as heat conduction problems [19,20], acoustic-structural interaction [21], potential flow [22,23], inclusions problems [24], coating structures [25], shape optimization [26], etc.

In this paper, we will apply the isogemoetric boundary element method to heat transfer problems with heat source. Since the introduction of heat source in the IGABEM, domain integral term will appear and cause the IGABEM to lose its advantage of having only boundary integrals. Up to now, there are several methods available to transform domain integrals into equivalent boundary integrals [27–30]. Here, we will adopt the radial integration method (RIM) (proposed by Gao [30]) to solve the domain integrals existing in the IGABEM. In the analysis of electronic devices, near-singular integral caused by the multi-scale structures exists in the present method. To improve the computation accuracy and efficiency, the hybrid nearly singular integration method proposed in [31] is used in this work. In addition, the method of subdomains is applied on problems of heat conduction in a body having different coefficients of thermal conductivity in two or more subregions.

The content of this paper is outlined as follows. In Section 2, a brief introduction of boundary element method for heat transfer problems with heat source is given. Section 3 introduces how the domain integrals can be transformed into boundary integral in IGABEM. The implementation of isogeometric boundary element method is given in Section 4. In Section 5, the method of subdomains is introduced to simulate multilayered problems in electronic packaging problems. Then, several numerical examples are discussed in Section 6, and we close with some concluding remarks in Section 7.

2. Introduction of the boundary integral equation with heat source

The governing equation of steady-state heat conduction in isotropic medium with internal heat source can be expressed as

$$k\frac{\partial}{\partial x_i}[\frac{\partial T(\mathbf{x})}{\partial x_i}]+b(\mathbf{x})=0, \mathbf{x}=(x_1,x_2)\in\Omega \tag{1}$$

where $i=1,2$, $T(\mathbf{x})$ represents the temperature at the point $\mathbf{x}$; k the thermal conductivity. $b(\mathbf{x})$ is the heat source and can be a constant or function of spatial coordinate $\mathbf{x}$; Ω the considered domain.

To solve these kinds of problems, the following boundary conditions should be given

$$T(\mathbf{x})=\bar{T}(\mathbf{x}), (\mathbf{x}\in\Gamma_1) \tag{2}$$

$$q(\mathbf{x})=-k\frac{\partial T(\mathbf{x})}{\partial \mathbf{n}}=\bar{q}(\mathbf{x}), (\mathbf{x}\in\Gamma_2) \tag{3}$$

in which q is the heat flux, $\bar{T}$ the known temperature on the boundary Γ_1, q the known heat flux on the boundary Γ_2. $\Gamma=\Gamma_1+\Gamma_2$ is the boundary of considered domain Ω; $\mathbf{n}=(n_1,n_2)$ the unit outward normal vector of boundary Γ.

For heat transfer problems with heat source in domian Ω, the boundary-domain integral equation can be derived as

$$c(\mathbf{y})u(\mathbf{y}) = -\int_\Gamma u^*(\mathbf{x},\mathbf{y})q(\mathbf{x})d\Gamma(\mathbf{x}) - \int_\Gamma q^*(\mathbf{x},\mathbf{y})u(\mathbf{x})d\Gamma(\mathbf{x}) + \int_\Omega u^*(\mathbf{x}',\mathbf{y})b(\mathbf{x}')d\Omega(\mathbf{x}') \tag{4}$$

where $\mathbf{y}=(y_1,y_2)\in\Gamma$ is the source point; $\mathbf{x}\in\Gamma$ denotes the field point; $\mathbf{x}'\in\Omega$ represents the point inside the considered domain. $c(\mathbf{y})$ is the geometric coefficient at the source point $\mathbf{y}$, which can be computed by $c(\mathbf{y})=1-\frac{\theta}{2\pi}$, where θ is the external angle of the boundary at point $\mathbf{y}$ [32]. $u(\mathbf{y})$ is the product of heat conduction coefficient and temperature at the source point $\mathbf{y}$, i.e. $u=kT$; $q(\mathbf{x})$ is the heat flux at the field point $\mathbf{x}$; $b(\mathbf{x})$ is the heat source at the field point $\mathbf{x}$. $u^*(\mathbf{x},\mathbf{y})$ and $q^*(\mathbf{x},\mathbf{y})$ are the fundamental solutions and can be expressed as

$$u^*(\mathbf{x},\mathbf{y})=-\frac{1}{2\pi}\ln r \tag{5}$$

$$q^*(\mathbf{x},\mathbf{y})=\frac{\partial u^*}{\partial \mathbf{n}}=\frac{\partial u^*}{\partial r}\frac{\partial r}{\partial \mathbf{n}}=-\frac{1}{2\pi r}\frac{\partial r}{\partial \mathbf{n}} \tag{6}$$

where $r=r(\mathbf{y},\mathbf{x})=||\mathbf{y}-\mathbf{x}||$ denotes the distance between the source point $\mathbf{y}$ and field point $\mathbf{x}$.

It can be seen that the solution of the integral equation in Eq. (4) only provides values of temperature (u) and flux (q) on the boundary Γ of the domain. Actually, after boundary quantities are obtained, the results at any point inside the computed domain can be readily computed by using a post-processing exercise, which is different from the finite element method. For the heat transfer problems in this work, the temperature at an interior point P_a can be simply computed by Eq. (7).

$$u(P_a) = -\int_\Gamma u^*(P_a,\mathbf{x})q(\mathbf{x})d\Gamma(\mathbf{x}) - \int_\Gamma q^*(P_a,\mathbf{x})t(\mathbf{x})d\Gamma(\mathbf{x}) + \int_\Omega u^*(\mathbf{x}',P_a)b(\mathbf{x}')d\Omega(\mathbf{x}') \tag{7}$$

3. Transform domain integral into boundary integral in IGABEM

In the process of solving heat transfer problems with heat source by IGABEM, domain integrals appear in the integral representation of Eqs. (4) and (7), which spoils the pure boundary character of the method. In this section, we will give a brief introduction how a domain integral can be transformed into boundary integral by radial integration method [33].

For a general function $f(\mathbf{x})$, its domain integral in Ω (bounded by Γ) can be described as [33]

$$\int_\Omega f(\mathbf{x})d\Omega=\int_\Gamma \frac{1}{r^\alpha(Q)}\frac{\partial r}{\partial \mathbf{n}}F(Q)d\Gamma\ (Q\in\Gamma) \tag{8}$$

in which

$$F(Q)=\int_0^{r(Q)} f(\mathbf{x})r^\alpha(Q)dr \tag{9}$$

where $\alpha=1$ for 2D problems and $\alpha=2$ for 3D problems.

For the boundary-domain integral equation shown in Eqs. (4) and (7), $f(x)=u^*(\mathbf{y},\mathbf{x}')b(\mathbf{x}')$, then the domain integral can be transformed into boundary integrals as

$$\int_\Omega u^*(\mathbf{y},\mathbf{x}')b(\mathbf{x}')d\Omega(\mathbf{x}')=\int_\Gamma \frac{1}{r^\alpha(\mathbf{y},\mathbf{x}^Q)}\frac{\partial \mathrm{r}}{\partial \mathbf{n}}F(\mathbf{y},\mathbf{x}^Q)d\Gamma(\mathbf{x}) \tag{10}$$

where

$$F(\mathbf{y},\mathbf{x}^Q)=\int_0^{r(\mathbf{y},\mathbf{x}^Q)} u^*(\mathbf{y},\mathbf{x}')b(\mathbf{x}')r^\alpha dr \tag{11}$$

in which $r(\mathbf{y},\mathbf{x}^Q)$ is the distance from source point $\mathbf{y}$ to boundary point $\mathbf{x}^Q$ and r represents the distance from source point $\mathbf{y}$ to field point $\mathbf{x}'$ inside the domain, as shown in Fig. 1. It should be noted that the degree of the NURBS basis functions for the geometry in Fig. 1 is $p=2$. And there are four knot spans (or elements) in the figure. The control points which defines control mesh can be used to describe the boundary of considered curve. In the present work, control points are multiplied by basis functions and summed to construct geometrical objects. The coordinate x_i ($i=1,2$) of any point can be expressed in terms of the distance r as follows:

$$x_i'=y_i+r_{,i}r(\mathbf{y},\mathbf{x}') \tag{12}$$

$$r_{,i}=\frac{\partial r}{\partial x_i}=\frac{x_i'-y_i}{r(\mathbf{y},\mathbf{x}')} \tag{13}$$

It should be pointed out that quantities $r_{,i}$ and y_i are constants for the radial integral in Eq. (11). And the boundary integral in Eq. (10) can be evaluated by the regular Gauss integration formula.

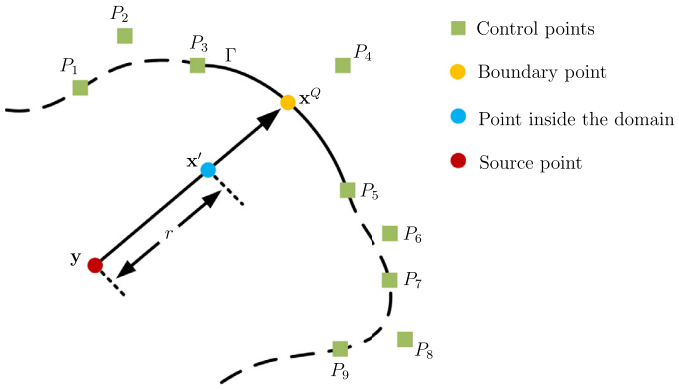

Fig. 1. Relationships among source point, field point and boundary point.

By substituting Eq. (10) into the boundary-domain integral Eq. (8), and we obtain a pure boundary integral equation

$$c(\mathbf{y})u(\mathbf{y}) = -\int_\Gamma u^*(\mathbf{y},\mathbf{x})q(\mathbf{x})d\Gamma(\mathbf{x}) - \int_\Gamma q^*(\mathbf{y},\mathbf{x})t(\mathbf{x})d\Gamma(\mathbf{x}) + \int_\Gamma \frac{1}{r^\alpha(\mathbf{y},\mathbf{x}^Q)}\frac{\partial r}{\partial \mathbf{n}}F(\mathbf{y},\mathbf{x}^Q)d\Gamma(\mathbf{x}^Q) \tag{14}$$

It should be noted that t and q are the coefficients at control points in Eq. (14). For the treatment of boundary conditions, the coefficients t (or q) can be expressed in terms of quantities $\bar{t}$ (or $\bar{q}$) at real boundary (collocation point) by pre-multiplying with inverse of $\mathbf{R}$

$$t = \mathbf{R}^{-1}\bar{t} \quad \text{or} \quad q = \mathbf{R}^{-1}\bar{q} \tag{15}$$

where $t = [t_1, t_2, t_3]^T$, $q = [q_1, q_2, q_3]^T$, $\bar{t} = [\bar{t}_1, \bar{t}_2, \bar{t}_3]^T$, $\bar{q} = [\bar{q}_1, \bar{q}_2, \bar{q}_3]^T$ and $\mathbf{R}$ is assembled from element contributions

$$\mathbf{R} = \begin{bmatrix} R_1(\xi_1) & R_2(\xi_1) & R_3(\xi_1) \\ R_1(\xi_2) & R_2(\xi_2) & R_3(\xi_2) \\ R_1(\xi_3) & R_2(\xi_3) & R_3(\xi_3) \end{bmatrix} \tag{16}$$

in which ξ_i $(i = 1, 2, 3)$ is the ith parameter value of collocation point and $R_j(\xi_i)$ $(i = 1, 2, 3;\ j = 1, 2, 3)$ represents the basis functions for a knot span.

4. Implementation of isogeometric boundary element method

Unlike the conventional boundary element method, in which the curves/surfaces and solution variables are defined using Lagrange polynomials, the IGABEM uses spline basises to describe them. In this work, the IGABEM based on NURBS basis function is used.

In this paper, we focus our attention on the application of IGABEM on heat transfer problems with heat source. Therefore, only a brief introduction of NURBS is given here. More details about NURBS can be found in literature [34].

A pth degree NURBS basis function $R_{a,p}(\xi)$ can be defined by a set of B-splines as

$$R_{a,p}(\xi) = \frac{N_{a,p}(\xi)w_a}{\sum_{i=1}^{p+1} N_{i,p}(\xi)w_i} \tag{17}$$

where w_i is a weight associated with control point $\mathbf{P}_i$. B-splines $N_{a,p}$ is a group of polynomials and defined by the following 'knot vector'

$$\Xi = \{\xi_0, \xi_1, \xi_2, \ldots, \xi_m\} \tag{18}$$

in which $m + 1$ is the number of knots. The B-spline basis functions of degree $p = 0$ are defined as

$$N_{a,0}(\xi) = \begin{cases} 1, & \text{if } \xi_a \le \xi < \xi_{a+1} \\ 0, & \text{otherwise,} \end{cases} \tag{19}$$

and, for $p = 1, 2, 3, \ldots$

$$N_{a,p}(\xi) = \frac{\xi - \xi_a}{\xi_{a+p} - \xi_a}N_{a,p-1}(\xi) + \frac{\xi_{a+p+1} - \xi}{\xi_{a+p+1} - \xi_{a+1}}N_{a+1,p-1}(\xi) \tag{20}$$

where ξ is a value in parameter space; a denotes the knot index. Let $n + 1$ be the number of basis functions or control points. Then the degree, p, number of control points, $n + 1$, and number of knots, $m + 1$, are related by $m = n + p + 1$.

In the implementation of IGABEM, the boundary Γ of considered model will be discretized into N_e isogeometric elements $\Gamma_e, e = 1, 2, \ldots, N_e$ which can be described by knot spans $[\xi_i, \xi_{i+1}]$, $\xi_i, \xi_{i+1} \in \Xi$. Based on the description of NURBS curve/surface in [34], the coordinate $(\mathbf{x}(\xi))$ of any point in the eth isogeometric element can be expressed as

$$\mathbf{x}(\xi) = \sum_{a=1}^{p+1} R_{a,p}(\xi)\mathrm{P}_a \tag{21}$$

where $\mathrm{P_a}$ is the control point; $R_{a,p}$ is the ath NURBS basis functions related to $\mathrm{P_a}$.

Similarly, the temperature and flux density fields at an element can be expressed using a NURBS expansion, i.e.

$$t(\xi) = \sum_{a=1}^{p+1} R_{a,p}(\xi)\tilde{t}_a \tag{22}$$

$$q(\xi) = \sum_{a=1}^{p+1} R_{a,p}(\xi)\tilde{q}_a \tag{23}$$

where $\tilde{t}_a$ and $\tilde{q}_a$ are the local temperature and flux parameters associated with the control point with index a, respectively. For IGABEM, NURBS basis functions are used to replace the classical polynomial formulations. Due to the non-interpolatory property of the NURBS (control point might not lie on the real boundary), $\tilde{t}_a$ and $\tilde{q}_a$ are just coefficients of temperature and flux and not nodal values, which is different from the classical BEM techniques. It should be noted that when all of the weights are of equal value for NURBS, the $\tilde{t}_a$ and $\tilde{q}_a$ will be the real temperature and flux.

Substituting the temperature and flux density fields at an element in Eqs. (22) and (23) into Eq. (14) results in the following discretised boundary integral equation:

$$\begin{aligned} c(\zeta_c)\sum_{l=1}^{p+1} N_l^{e_0}(\zeta_c)\tilde{t}^{le_0} = &-\sum_{e=1}^{N_e}\sum_{l=1}^{p+1}\left[\int_{-1}^{1} u^*(\zeta_c,\hat{\xi})N_l^e(\hat{\xi})J(\hat{\xi})d\hat{\xi}\right]\tilde{q}^{le} \\ &-\sum_{e=1}^{N_e}\sum_{l=1}^{p+1}\left[\int_{-1}^{1} q^*(\zeta_c,\hat{\xi})N_l^e(\hat{\xi})J(\hat{\xi})d\hat{\xi}\right]\tilde{t}^{le} \\ &+\sum_{e=1}^{N_e}\left[\int_{-1}^{1}\frac{1}{r^\alpha(\zeta_c,\hat{\xi})}\frac{\partial r}{\partial \mathbf{n}}F(\zeta_c,\hat{\xi})J(\hat{\xi})d\hat{\xi}\right] \end{aligned} \tag{24}$$

where c represents the collocation point index; ζ_c is the parameter coordinate of the collocation point c; $\hat{\xi}$ is the Gaussian integral space, $\hat{\xi} \in [-1, 1]$; $\tilde{t}^{le}$ and $\tilde{q}^{le}$ are the physical quantity coefficients of temperature and heat flow on element e, respectively. J is the Jacobian of transformation from the isogeometric element $([\xi_i, \xi_{i+1}])$ to parent element:

$$J(\hat{\xi}) = \frac{d\Gamma}{d\hat{\xi}} = \frac{d\Gamma}{d\xi}\frac{d\xi}{d\hat{\xi}} \tag{25}$$

If the boundary integral equation is applied for all the collocation points produced by Greville abscissae [35], Eq. (24) can form the matrix form as follows:

$$\mathbf{Ht} = \mathbf{Gq} + \mathbf{y}_b \tag{26}$$

where $\mathbf{H} = [H_{ij}]$ and $\mathbf{G} = [G_{ij}]$ are coefficient matrix with

$$H^{ij} = \int_{-1}^{1} q^*(\zeta_c,\hat{\xi})N_l^e(\hat{\xi})J(\hat{\xi})d\hat{\xi} \tag{27}$$

$$G^{ij} = \int_{-1}^{1} u^*(\zeta_c,\hat{\xi})N_l^e(\hat{\xi})J(\hat{\xi})d\hat{\xi} \tag{28}$$

In the analysis of electronic devices, near-singular integral caused by the multi-scale structures exists in the present method. Recently, literature [31] proposed an effective method (sinh$^+$ scheme) to compute the nearly singular integrals in IGABEM by combining the benefits of the sinh transformation (of, amongst others, Gu et al. [36]) and adaptive integration scheme (of Gao and Davies [37]). To improve the computation accuracy and efficiency in this work, the integration method proposed in [31] is adopted.

In the implementation of the sinh$^+$ scheme, the aspect ratio $d^* = d/L$ which describes the proximity of the source point to the element is defined, where d represents the minimum distance from the source point to the considered element and L is the length of the element. For the computation of an integral, when the aspect ratio d^* is greater than the given critical aspect ratio d^*_{crit}, there is no near-singularity for the current integral and the adaptive integration method is applied. When $d^* < d^*_{\text{crit}}$, the near-singularity triggers a hybrid integration scheme (named sinh$^+$). In the computation of the nearly singular integrals with knot span $[\xi_i, \xi_{i+1}]$, the knot span will be subdivided into three parts by the truncation error E_{trun} of Taylor expansion in predicting the square distance. For the sub-region with $E_{\text{trun}} < eps$, the sinh transformation method is adopted. The adaptive integral method will be used to compute the integrals on the subdivisions with $E_{\text{trun}} > eps$. Here, eps is a given error tolerances.

Applying boundary conditions to Eq. (26), a linear system equation is formed as follows:

$$\mathbf{A}\boldsymbol{\lambda} = \mathbf{b} \tag{29}$$

where matrix $\mathbf{A}$ contains the integral values related to the unknown temperature and heat flux, $\boldsymbol{\lambda}$ includes the unknown temperature and heat flux, and $\mathbf{b}$ is a column vector composed of known quantities. The unknown temperature and heat flux on the boundary can be obtained by solving Eq. (29). By substituting these obtained (and known) temperatures and heat fluxes on the boundary into Eq. (7), the internal temperature of the model can be obtained.

5. IGABEM in multilayer structure

The solution procedures described above are applicable to homogeneous domains, as the fundamental solutions used assume that material properties do not change inside the domain being analysed. In electronic packaging structures, there might be various layers/inclusions with different properties. For multilayered structures which are connected to each other, each region is treated in the same way as discussed previously but can now be assigned different material properties by subregion IGABEM method. Actually, the piecewise homogeneous material in electronic packaging structures can be analyzed easily by this method.

Due to the physical quantities at the interface between two regions are unknown, the number of unknowns is increased and additional conditions at interfaces are required to solve the problem. These conditions are written as:

$$t^n = t^{n+1}, q^n = -q^{n+1} \tag{30}$$

where the superscripts n and $n+1$ denote the number index of two-layer regions with a common interface. For a model with three subregions (region 1 is a chip layer), we can obtain following matrix equations:

$$\mathbf{H}^1\mathbf{t}^1 = \mathbf{G}^1\mathbf{q}^1 + \mathbf{y}_b \tag{31}$$

$$\mathbf{H}^2\mathbf{t}^2 = \mathbf{G}^2\mathbf{q}^2 \tag{32}$$

$$\mathbf{H}^3\mathbf{t}^3 = \mathbf{G}^3\mathbf{q}^3 \tag{33}$$

To solve this problem, the following relationships along the interface should be given

$$\mathbf{t}^1 = \mathbf{t}^2, \mathbf{q}^1 = -\mathbf{q}^2 \tag{34}$$

$$\mathbf{t}^2 = \mathbf{t}^3, \mathbf{q}^2 = -\mathbf{q}^3 \tag{35}$$

According to boundary conditions, unknown quantities (including quantities at the interface) can be obtained by solving linear equations for all regions.

6. Numerical examples

In this section, through several numerical examples the accuracy of the IGABEM for heat transfer problems are demonstrated. To carry out the accuracy analysis, an average relative error is given as

$$\text{RE} = \frac{|f_{\text{num}} - f_{\text{ref}}|}{|f_{\text{ref}}|} \tag{36}$$

where f_{num} is the result obtained by proposed method, and f_{ref} represents the reference solution. The models in this work are described by quadratic NURBS curves with knot vector $\Xi = \{0, 0, 0, 1, 1, 2, 2, 3, 3, 4, 4, 4\}$. Unit weights ($w_i \equiv 1$) are used for square boundary. And the following weights are adopted for circular boundary.

$$w = [1, \frac{\sqrt{2}}{2}, 1, \frac{\sqrt{2}}{2}, 1, \frac{\sqrt{2}}{2}, 1, \frac{\sqrt{2}}{2}, 1]$$

6.1. Thermal analysis of rectangular region with heat source

Here, a 1 mm × 1 mm square plate with heat source is calculated by present IGABEM. The upper and lower boundary are insulated, i.e. $\partial T/\partial \mathbf{n} = 0$; The left and right boundary temperatures are 100 °C and 200 °C, respectively. The thermal conductivity is 1 W/(m · K), and the internal heat source $Q(x)$ is a constant of 500 W/m^2. The exact solutions determined by boundary conditions and heat sources are as follows.

$$T = -250x^2 + 350x + 100 \tag{37}$$

Fig. 2 (a) shows the relative error surface of computated results for the temperature when $Q(x) = 500$ W/m^2. It can be seen that the proposed method is very accurate (relative error is less than 4‰) even only four isogeometric boundary elements is used. When the internal heat source $Q(x)$ is selected as $700e^{-0.5(x^2+y^2)}$, the temperature distribution is given in Fig. 2.

6.2. 'Sandwich' structure in IGBT

In this example, a 'Sandwich' structure (including chip layer, solder layer and upper copper layer) in IGBT is studied to assess the applicability of the present IGABEM on steady state heat transfer in multiply connected domain. As shown in Fig. 3 the upper and lower boundary temperatures are given as $T_U = 150$°C and $T_L = 10$°C, respectively. The left and right boundaries are insulated, and the heat source in the chip layer is 2000 W/m^2. Thermal conductivities of upper, middle and lower layers are 1 W/(m · K), 20 W/(m · K) and 1 W/(m · K). The geometry size of the model is given as $a = 1$ mm, $b_1 = 0.3$ mm, $b_2 = 0.15$ mm and $b_3 = 0.3$ mm. Fig. 4(a) shows the temperature obtained by present IGABEM. For comparison, the contour plot of the reference results (obtained by ABAQUS) is also given in Fig. 4(b). From Fig. 4(a) and 4(b), it can be seen that the computational results are in good agreement with the reference results.

Fig. 5 shows the numerical results of temperature when the computed points are moving along the curve $(0.5, y)$, and reference solutions (obtained by ABAQUS) are given as comparison. From Fig. 5, we can clearly see that the current solutions are in good agreement with the reference results, which means that the present scheme is effective for the numerical analysis of IGBT devices.

Here a simplified IGBT model is analysed by the present IGABEM. The thickness of chip layer and copper layer is selected as 0.3 mm and the thickness of solder layer is selected as 0.15 mm. The thermal conductivities of chip layer, solder layer and upper copper layer are 147 W/(m · K), 57 W/(m · K), and 400 W/(m · K). The temperatures on bottom and top sides are prescribed as 80 °C and 70 °C, respectively. The

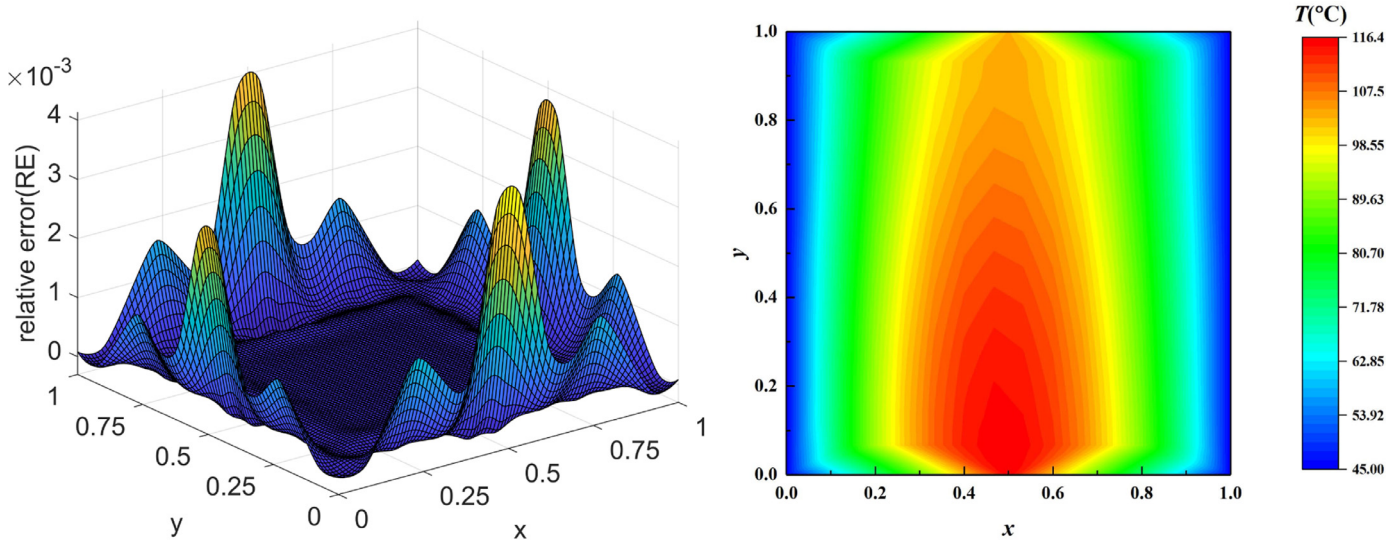

Fig. 2. Temperature distribution and relative errors computed by the present IGABEM.

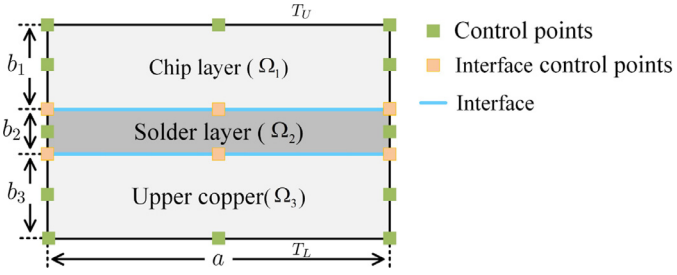

Fig. 3. DBC model of IGBT device.

chip layer involves heat source with 650W/m^2. Fig. 6 shows the temperature distribution. When the heat release rate of the chip is a function as $450(x^2 + y^2)$, Fig. 7 gives the temperature distribution for the whole model.

To further study the influence of thickness of chip on temperature distribution, the thickness b_1 of the chip will be taken as 0.15 mm, 0.2 mm, 0.25 mm and 0.3 mm. The temperature distribution along the parameter curve $(0.5, y)$ under different chip thicknesses are given in Fig. 8. It can be seen from Fig. 8 that maximum temperature of the structure occurs in the chip layer. And the values of maximum temperature are also given in Fig. 8.

6.3. Heat transfer through multilayer cylinder with heat source

In this example we study the heat transfer through a cylinder with multilayer structures as shown in Fig. 9.

For this model, the power density inside the model is 100 W/m^2, the location of heat source is shown in Fig. 9. As shown in the figure, temperatures on the inner and outer diameters are prescribed as boundary conditions, being $T_1 = 200°C$ and $T_2 = 80°C$. Thermal conductivities of the inner layer, the intermediate layer and the outer layer are selected as 1 W/(m · K), 22 W/(m · K) and 0.23 W/(m · K).

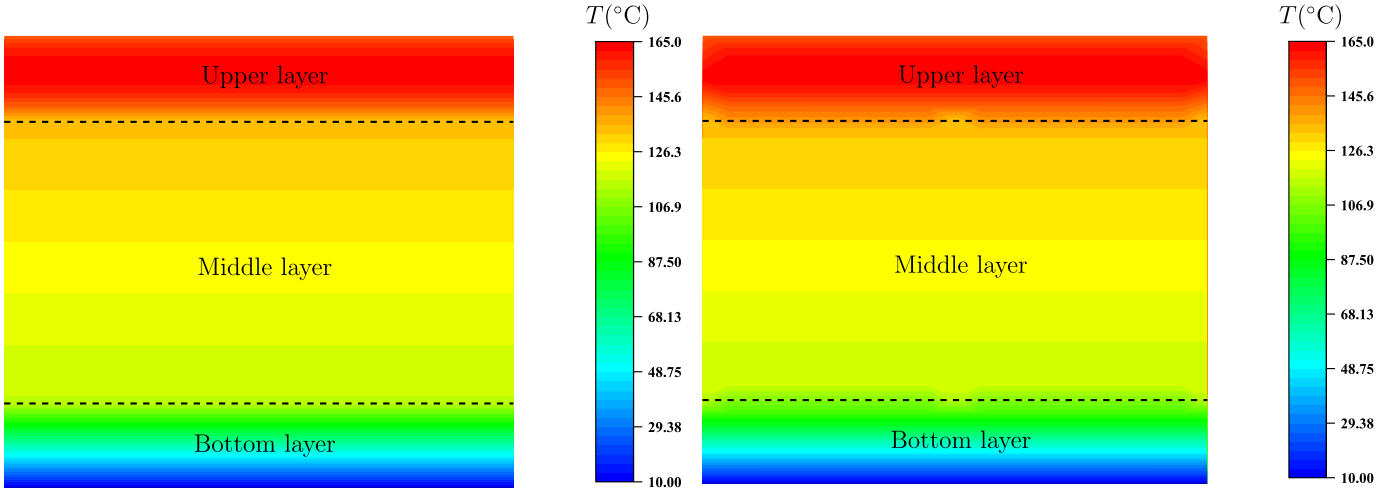

Fig. 4. Temperature results obtained by IGABEM and ABAQUS.

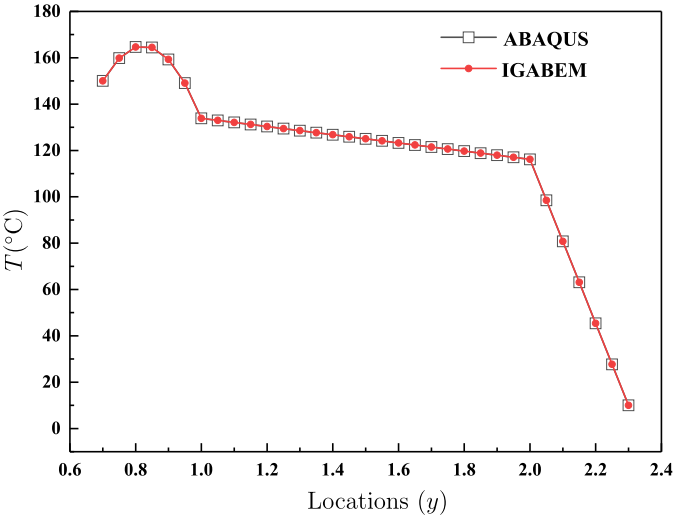

Fig. 5. Comparison of temperature distribution for the present results and the reference (FEM) solutions along $(0.5, y)$.

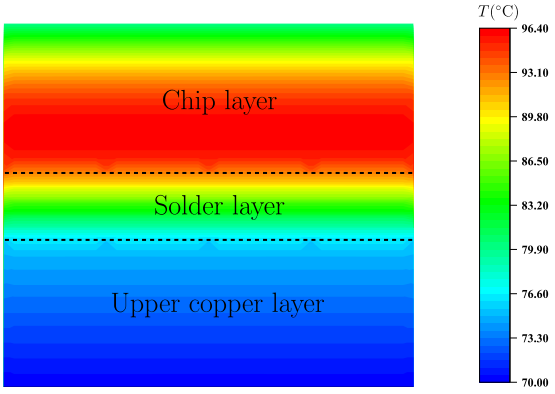

Fig. 6. Temperature distribution in DBC of IGBT.

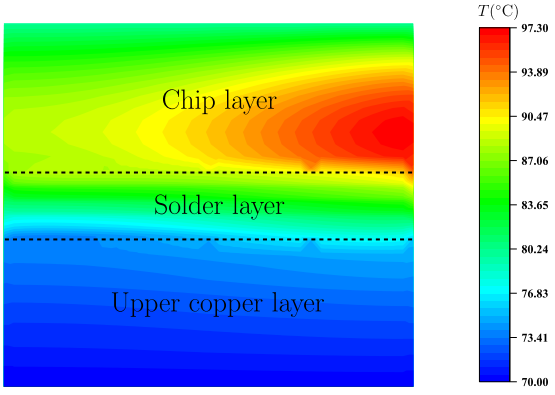

Fig. 7. Temperature distribution in DBC of IGBT when heat source is $450(x^2 + y^2)$.

In the computation of IGABEM, 32 isogeometric boundary elements are used to discretise the whole model. Here, a finite element model is also constructed with the FEM software (ABAQUS) to offer a reference solution. The mesh consists of 1443 elements and 1505 nodes. Fig. 10 shows relative errors of temperature at 634 selected points. As can be seen from Fig. 10, the peak value of the error surface is 1.5‰, which means that the results are in good agreement with the FEM solutions for this model.

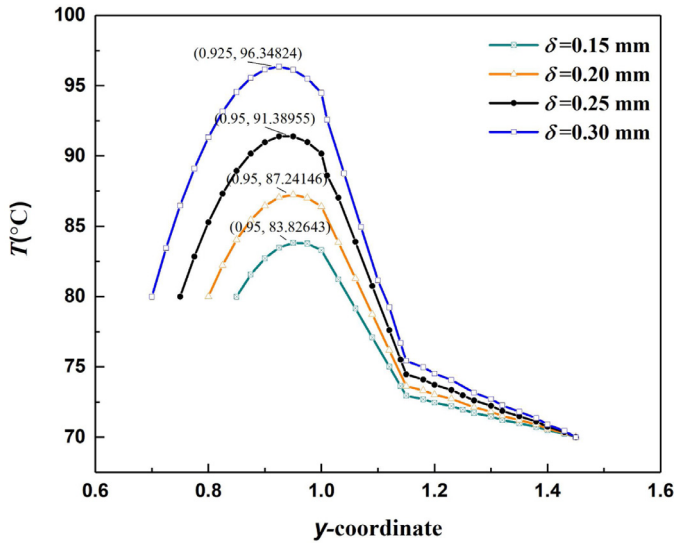

Fig. 8. Temperature distribution along curve $(0.5, y)$ with different chip thicknesses.

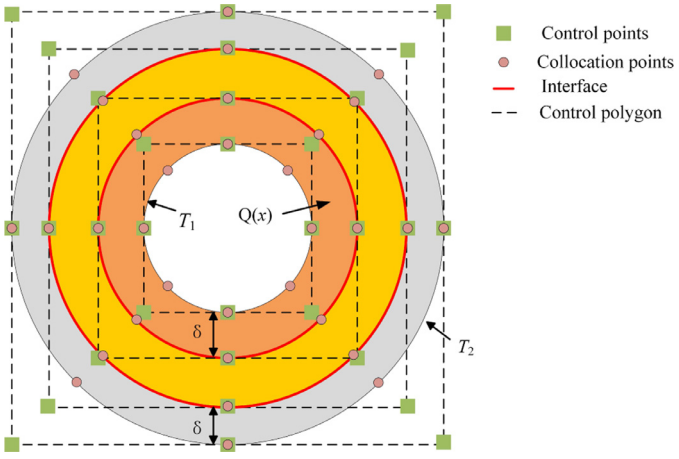

Fig. 9. cylinder model with multilayer structures.

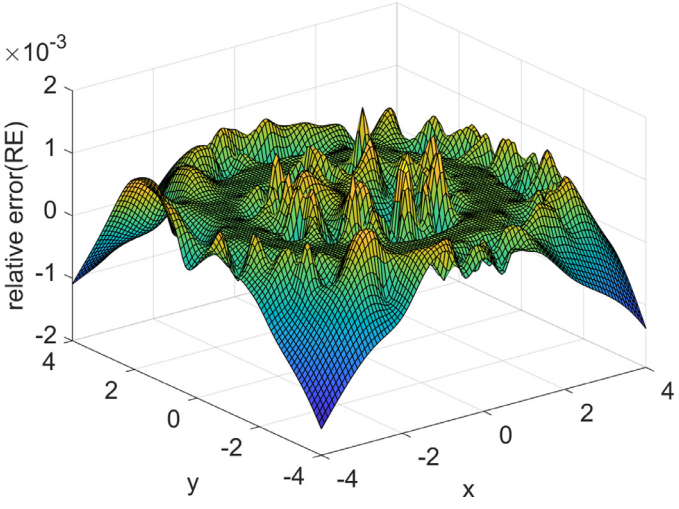

Fig. 10. Relative errors of computed points.

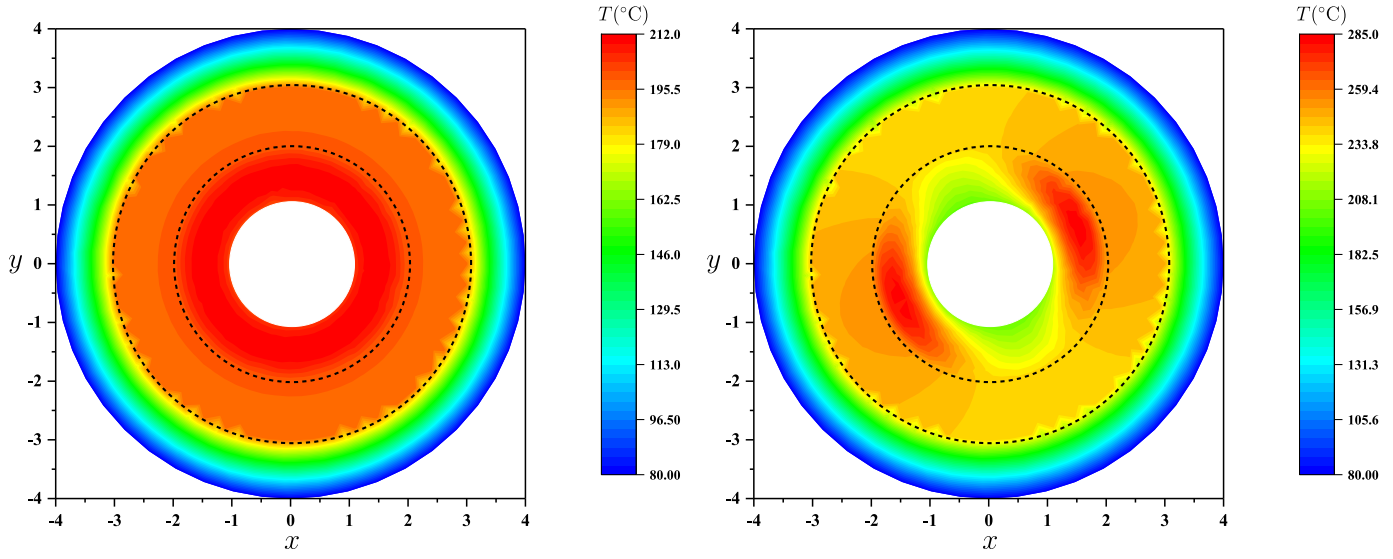

(a) heat source is selected as $100\mathrm{W}/(\mathrm{m}\cdot\mathrm{K})$ (b) heat source is selected as $700(x^2+xy)$

Fig. 11. Temperature distribution with different heat sources.

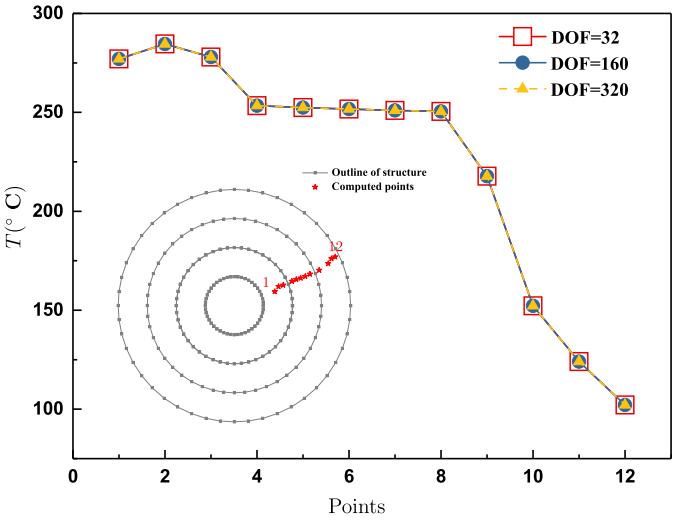

Fig. 12. values of temperature obtained by different DOF.

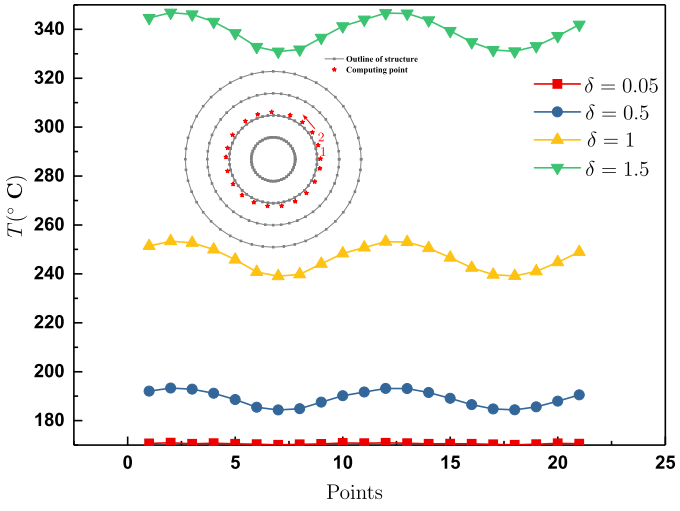

Fig. 13. Temperature results for different δ.

Fig. 11 (a) and 11(b) shows the temperature distribution for different heat sources. It can be seen from Fig. 11(a) that the temperature of the inner layer with heat source is the highest and gradually reduce from the inner layer to the outer layer. It can be seen from Fig. 11(b) that the highest temperature is concentrated on both sides of the inner layer, and the temperature gradually decreases from the inner layer to the outer layer.

We take 12 points along the red curve in Fig. 12 as our evaluation points. Fig. 12 also shows the numerical values of temperature under different DOF, which indicates that accurate results can be obtained without refinement for the model.

To further study the influence of thickness δ (shown in Fig. 9) on temperature, temperature results for different values of δ are shown in Fig. 13. The computed points inside the model lying on the contour S_1, which is defined by

$$S_1 = \{(x,y); x = r_0\cos\theta, y = r_0\sin\theta, r_0 = 2.15\mathrm{mm}, \theta \in [0, 2\pi]\} \quad (38)$$

It can be seen that the temperature along S_1 changes in a wavy manner. While $\delta = 0.05$, temperature variation is not obvious, which is resulted from the heat provided by the heat source is very small.

7. Conclusion

In this paper, the isogeometric boundary element method is used to study heat transfer problems with heat source. Since only the boundary of each material is considered, therefore there is no need for domain meshing and internal unknowns, which enables fast calculation for multilayer problems, especially for semiconductor models. However, in some engineering problems for semiconductor structure, heat release of chip which can be seen as heat source will result in domain integrals in the computation. In this work, we apply the radial integration method to handle domain integrals resulted from heat sources.

To offer a reference solution, several finite element models are constructed by means of the ABAQUS. We compared the present results with those obtained by FEM. The given numerical examples have demon-

strated the correctness and effectiveness of the developed method for some electronic devices.

Declaration of Competing Interest

None.

Acknowledgments

The research was supported by the National Natural Science Foundation of China (No. 12002009), the General Program of Science and Technology Development Project of Beijing Municipal Education Commission (No. KM202110005032), General Program of Science and Technology Development Project of BJUT and Beijing Postdoctoral Research Foundation.

References

[1] Cundapı R, Moya S, Cazarez O. Analytical solution of the transient heat conduction in the absorber tube of a parabolic trough solar collector under quasi-steady conditions. J Sol Energy Eng Trans ASME 2021;143(3).
[2] Azizul FM, Alsabery AI, Hashim I, Chamkha AJ. Impact of heat source on combined convection flow inside wavy-walled cavity filled with nanofluids via heatline concept. Appl Math Comput 2021;393:125754.
[3] Lee KY, Lee TS. Hygrothermal fracture analysis of plastic IC package in reflow soldering process. Trans Korean Soc Mech Eng A 1996;121(3):148–55.
[4] Raszkowski T, Zubert M. Analysis of algorithm efficiency for heat diffusion at nanoscale based on a MEMS structure investigation. Energies 2020;13(10):2520.
[5] Dong C, Lee KY. Stress analysis of plastic IC package containing various interface delaminations using the boundary element method. Eng Fract Mech 2008;75(1):1–16.
[6] Mera NS, Elliott L, Ingham DB, Lesnic D. Singularities in anisotropic steady-state heat conduction using a boundary element method. Int J Numer Methods Eng 2002;53(10):2413–27.
[7] Khatir Z, Lefebvre S. Boundary element analysis of thermal fatigue effects on high power IGBT modules. Microelectron Reliab 2004;44(6):929–38.
[8] Shiah Y, Chang R-Y, Hematiyan M. Three-dimensional analysis of heat conduction in anisotropic composites with thin adhesive/interstitial media by the boundary element method. Eng Anal Bound Elem 2021;123:36–47.
[9] Škerget L, Tadeu A, António J. Numerical simulation of heat transport in multilayered composite pipe. Eng Anal Bound Elem 2020;120:28–37.
[10] Vallepuga-Espinosa J, Ubero-Martínez I, Rodríguez-Tembleque L, Cifuentes-Rodríguez J. A boundary element procedure to analyze the thermomechanical contact problem in 3d microelectronic packaging. Eng Anal Bound Elem 2020;115:28–39.
[11] Majchrzak E, Turchan L. Modeling of laser heating of bi-layered microdomain using the general boundary element method. Eng Anal Bound Elem 2019;108:438–46.
[12] Gu Y, Zhang C. Novel special crack-tip elements for interface crack analysis by an efficient boundary element method. Eng Fract Mech 2020;239:107302.
[13] Hughes T, Cottrell J, Bazilevs Y. Isogeometric analysis: CAD, finite elements, NURBS, exact geometry and mesh refinement. Comput Methods Appl Mech Eng 2005;194(39):4135–95.
[14] Liu Z, Yang M, Cheng J, Wu D, Tan J. Meta-model based stochastic isogeometric analysis of composite plates. Int J Mech Sci 2021;194:106194.
[15] Kumar D, Poh LH, Quek ST. Isogeometric shape optimization of missing rib auxetics with prescribed negative Poisson's ratio over large strains using genetic algorithm. Int J Mech Sci 2021;193:106169.
[16] Chen L, Li B, de Borst R. Adaptive isogeometric analysis for phase-field modeling of anisotropic brittle fracture. Int J Numer Methods Eng 2020;121(20):4630–48.
[17] Yu T, Chen B, Natarajan S, Bui TQ. A locally refined adaptive isogeometric analysis for steady-state heat conduction problems. Eng Anal Bound Elem 2020;117:119–31.
[18] Simpson R, Bordas S, Trevelyan J, Rabczuk T. A two-dimensional isogeometric boundary element method for elastostatic analysis. Comput Methods Appl Mech Eng 2012;209–212:87–100.
[19] Yu B, Cao G, Huo W, Zhou H, Atroshchenko E. Isogeometric dual reciprocity boundary element method for solving transient heat conduction problems with heat sources. J Comput Appl Math 2021;385:113197.
[20] Zang Q, Liu J, Ye W, Lin G. Isogeometric boundary element method for steady-state heat transfer with concentrated/surface heat sources. Eng Anal Bound Elem 2021;122:202–13.
[21] Wu Y, Dong C, Yang H, Sun F. Isogeometric symmetric fe-be coupling method for acoustic-structural interaction. Appl Math Comput 2021;393:125758.
[22] Chouliaras S, Kaklis P, Kostas K, Ginnis A, Politis C. An isogeometric boundary element method for 3d lifting flows using t-splines. Comput Methods Appl Mech Eng 2021;373:113556.
[23] Han Z, Huang Y, Cheng C, Liang Y, Hu Z, Niu Z. The semianalytical analysis of nearly singular integrals in 2d potential problem by isogeometric boundary element method. Int J Numer Methods Eng 2020;121(16):3560–83.
[24] Beer G, Dünser C, Ruocco E, Mallardo V. Efficient simulation of inclusions and reinforcement bars with the isogeometric boundary element method. Comput Methods Appl Mech Eng 2020;372:113409.
[25] Gong Y, Dong C, Qin F, Hattori G, Trevelyan J. Hybrid nearly singular integration for three-dimensional isogeometric boundary element analysis of coatings and other thin structures. Comput Methods Appl Mech Eng 2020;367:113099.
[26] Mostafa Shaaban A, Anitescu C, Atroshchenko E, Rabczuk T. Shape optimization by conventional and extended isogeometric boundary element method with PSO for two-dimensional Helmholtz acoustic problems. Eng Anal Bound Elem 2020;113:156–69.
[27] Neves AC, Brebbia CA. The multiple reciprocity boundary element method in elasticity: a new approach for transforming domain integrals to the boundary. Int J Numer Methods Eng 1991;31(4):709–27.
[28] Ma H, Kamiya N, Xu SQ. Complete polynomial expansion of domain variables at boundary for two-dimensional elasto-plastic problems. Eng Anal Bound Elem 1998;21(3):271–5.
[29] Takhteyev V, Brebbia C. Analytical integrations in boundary elements. Eng Anal Bound Elem 1990;7(2):95–100.
[30] Gao X-W. The radial integration method for evaluation of domain integrals with boundary-only discretization. Eng Anal Bound Elem 2002;26(10):905–16.
[31] Gong Y, Trevelyan J, Hattori G, Dong C. Hybrid nearly singular integration for isogeometric boundary element analysis of coatings and other thin 2d structures. Comput Methods Appl Mech Eng 2019;346:642–73.
[32] Gong Y, Dong C, Qu X. An adaptive isogeometric boundary element method for predicting the effective thermal conductivity of steady state heterogeneity. Adv Eng Softw 2018;119:103–15.
[33] Gao X-W. A meshless BEM for isotropic heat conduction problems with heat generation and spatially varying conductivity. Int J Numer Methods Eng 2006;66(9):1411–31.
[34] Piegl L, Tiller W. The NURBS book. Springer-Verlag Berlin Heidelberg; 1997.
[35] Johnson RW. Higher order b-spline collocation at the Greville abscissae. Appl Numer Math 2005;52(1):63–75.
[36] Gu Y, Gao H, Chen W, Zhang C. A general algorithm for evaluating nearly singular integrals in anisotropic three-dimensional boundary element analysis. Comput Methods Appl Mech Eng 2016;308:483–98.
[37] Gao X-W, Davies TG. Boundary element programming in mechanics. Cambridge University Press, New York; 2002.